

Short communication

Impedance analysis of PLD $\text{LiNi}_{0.8}\text{Co}_{0.2}\text{O}_2$ film electrode

N. Imanishi^{a,*}, K. Shizuka^a, T. Matsumura^a, A. Hirano^a, Y. Takeda^a, R. Kanno^b

^a Department of Chemistry, Mie University, 1577 Kurimamachiyacho, Tsu, Mie 514-8507, Japan

^b Tokyo Institute of Technology, 4259 Nagatsutacho, Midoriku, Yokohama 226-8503, Japan

Available online 3 July 2007

Abstract

The kinetics of intercalation are discussed using a pulsed laser deposition (PLD) film electrode and electrochemical impedance analysis. Films of $\text{LiNi}_{0.8}\text{Co}_{0.2}\text{O}_2$, deposited on single crystal substrates, were used for the study. The films have intercalative or blocking orientations on different crystal surfaces of the substrates. Impedance spectra show that there are at least three elemental processes in intercalation. Two processes at higher frequencies suggest that they occur at the electrode surface and are influenced by the orientation of the film. The third process appearing at low frequencies below 1 Hz indicates lithium motion in the bulk structure and shows the largest resistance among the three processes. This lithium conduction in a thin PLD film shows a semicircular response and is considered to be influenced more by the structure due to the nanometer-scale thickness.

© 2007 Elsevier B.V. All rights reserved.

Keywords: Intercalation; Impedance; Pulsed laser deposition; Epitaxial film

1. Introduction

Enhancement of electrode reaction speed is important in lithium ion batteries in order to develop novel high-power devices and to achieve high energy conversion efficiencies. Growing consciousness of safety concerns is also promoting research and development of all solid-state batteries. Since the reaction speed at the solid–solid interface is significantly slow, kinetic studies of the electrode reaction are gaining in importance.

The problem in kinetic studies using ceramic electrodes lies in the complexity of precisely describing structures of the electrode and the interface with the electrolyte. Structural parameters include the crystal structure of the material, the size of the primary particles, agglomeration of particles, distribution of electrode components, conduction paths of electrons and ions, and morphology of the interface. These parameters have an effect on each other and the reaction speed is determined as a total response including all of these parameters. The analysis of individual parameters is practically impossible and kinetic studies in many cases become empirical.

As one approach towards solving this problem, preparation of a pulsed laser deposition (PLD) film is beneficial under the con-

cept of simplification or idealization of the electrode system. It is possible to prepare oxides epitaxially on a single crystal substrate by laser ablation deposition [1–4]. The film forms as a single crystal or an oriented polycrystal, depending on the mismatch between the film and substrate. In both cases, however, the structure is much simpler and more appropriate for kinetic study than a conventional electrode system. The crystal orientation of the film can be controlled by the surface atomic structure of the substrate [1,4–6]. In this article, kinetic parameters of intercalation for a $\text{LiNi}_{0.8}\text{Co}_{0.2}\text{O}_2$ PLD electrode were measured by the electrochemical impedance method [7–11], and the effects of crystal orientation on these parameters are discussed.

2. Experimental

Atomic proportions of Li_2CO_3 , $\text{Ni}(\text{OH})_2$ and Co_3O_4 in 15:24:2, were weighed for the preparation of $\text{LiNi}_{0.8}\text{Co}_{0.2}\text{O}_2$. This mixture was calcined at 600 °C for 6 h. After milling the resultant material, it was fired again at a temperature of 725 °C for 24 h to complete the reaction. The structure was confirmed by XRD, and a sintered pellet of the material was used as a target for laser ablation deposition.

A single-crystal of Nb-doped SrTiO_3 (STO) was used as the substrate. The substrate also functions as a current collector for the working electrode. Flat square plates with dimensions of 10 mm × 10 mm × 0.5 mm were sliced from the ingot for (1 1 0)

* Corresponding author.

E-mail address: imanishi@chem.mie-u.ac.jp (N. Imanishi).

or (1 1 1) crystal planes of STO to appear. The flatness of the surface was less than 15 angstroms.

The ablation of $\text{LiNi}_{0.8}\text{Co}_{0.2}\text{O}_2$ was performed using a KrF excimer laser (248 nm). The laser power was adjusted to 250 mJ and the pulse irradiation frequency was 10 Hz. The substrate temperature was held at 600 °C during deposition. The oxygen pressure in the ablation chamber was maintained at 3.3 Pa. The distance between the substrate and the target was 7.5 cm. The deposition was carried out for 60 min.

The preparation and structural characterization of the epitaxial PLD films were carried out by Kanno and co-workers of Tokyo Institute of Technology. A paper giving details on the preparation and structural characterization is in preparation and will be published in the near future.

Impedance spectra were measured, in order to obtain kinetic information, using a Solartron 1260 Frequency Response Analyzer with a 1287 Electrochemical Interface. Three electrode test cells with lithium reference and counter electrodes were used for the measurements. The impedance measurements were carried out by applying 10 mV of ac current in the range of 10^6 – 10^{-3} Hz.

3. Results and discussion

Thin-film X-ray diffraction patterns were measured, as shown in Fig. 1, to discuss the crystal structure of the ablated films. The $\text{LiNi}_{0.8}\text{Co}_{0.2}\text{O}_2$ electrode on STO(1 1 0) shows a 110 diffraction peak near 60° in 2 θ . The active material in this case has intercalative orientation for lithium ions in the electrolyte. Another $\text{LiNi}_{0.8}\text{Co}_{0.2}\text{O}_2$ electrode on STO(1 1 1) shows a series of 00 l diffractions. Thus, the active material orders the basal planes parallel to the surface of the substrate. The film in this case shows a blocking effect against lithium intercalation. It was confirmed that these films are epitaxially grown on a single crystal substrate.

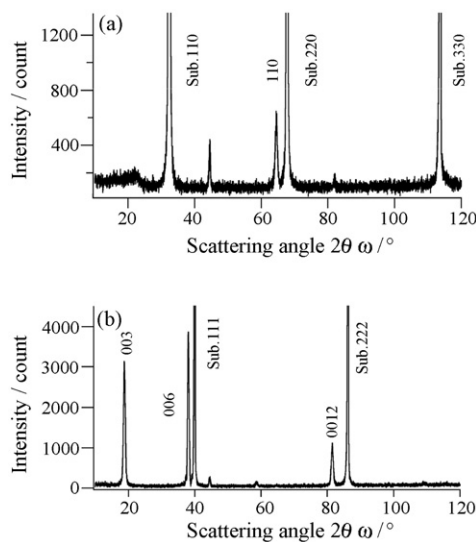


Fig. 1. XRD patterns of ablation films deposited on Nb-doped SrTiO₃ substrate. (a) $\text{LiNi}_{0.8}\text{Co}_{0.2}\text{O}_2$ film on (1 1 0) crystal plane of STO and denoted as an intercalative film. (b) $\text{LiNi}_{0.8}\text{Co}_{0.2}\text{O}_2$ film on (1 1 1) crystal plane of STO and denoted as a blocking film.

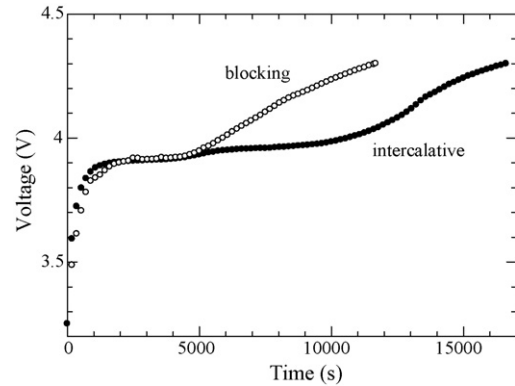


Fig. 2. Constant current charge curves of $\text{LiNi}_{0.8}\text{Co}_{0.2}\text{O}_2$ films on STO(1 1 0) and (1 1 1) substrates. The former is indicated as intercalative and the latter is indicated as blocking.

The charge profiles at a constant current density are shown in Fig. 2. The shapes and potentials of these curves are similar to those of the powder $\text{LiNi}_{0.8}\text{Co}_{0.2}\text{O}_2$ electrode. The difference in coulombic capacities is considered to occur by the different crystal orientations of the $\text{LiNi}_{0.8}\text{Co}_{0.2}\text{O}_2$ films.

Impedance spectra of $\text{LiNi}_{0.8}\text{Co}_{0.2}\text{O}_2$ electrodes on STO(1 1 0) and STO(1 1 1) in Fig. 3 shows similar profiles,

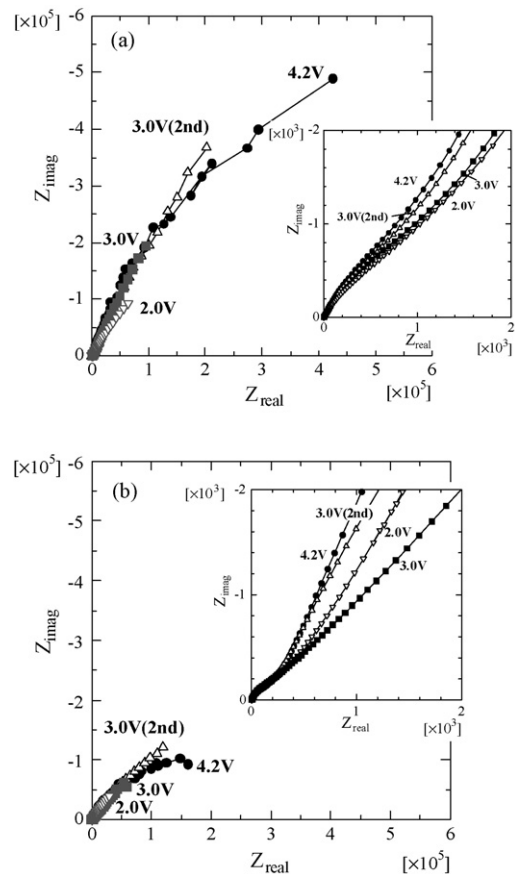


Fig. 3. Complex plane impedance plots for (a) $\text{LiNi}_{0.8}\text{Co}_{0.2}\text{O}_2$ films on STO(1 1 0) and (b) (1 1 1) substrates. The whole spectra show frequencies ranging from 10^6 to 10^{-3} Hz. The insets show the enlarged high frequency region. The numbers beside the curves show the potentiostatic equilibrated cell voltage.

wherein only less than half of a large semicircle appears in the frequency range from 1 MHz to 1 mHz. The insets in the figure show an enlarged high frequency region, and indicate another small semicircle for both samples. The total resistances roughly estimated from the spectra are on the order of $10^5 \Omega$. These unusually large values are partly attributed to small surface area of the electrodes. The electrode prepared by laser ablation has an extremely flat surface compared to a normal “mixed and pressed” electrode which is comprised of active material particles and other components such as acetylene black and so on.

Both electrodes show reversible size change of the spectra on the application of a potentiostatic charge and discharge. In the case of intercalative $\text{LiNi}_{0.8}\text{Co}_{0.2}\text{O}_2$ on $\text{STO}(1\ 1\ 0)$, it was initially equilibrated at 3.0 V versus lithium. Next, at 4.2 V, the semicircle became larger, and decreased alternatively when discharging to the initial potential of 3.0 V. It shows further small resistance by discharging to 2.0 V. The same pattern of spectral change was observed for the $\text{LiNi}_{0.8}\text{Co}_{0.2}\text{O}_2$ on $\text{STO}(1\ 1\ 1)$. This reversible change confirms a Faradaic reaction, that is, lithium intercalation mainly occurs in these ablation electrodes.

Comparison between spectra of intercalative and blocking $\text{LiNi}_{0.8}\text{Co}_{0.2}\text{O}_2$ electrodes shows a noticeable difference in their resistances. It is naturally expected that the blocking electrode will show much higher resistance due to the morphology preventing lithium ions from intercalation. The ideal blocking electrode indicates capacitive response which shows a straight upright line in the complex plane. However, the experimental data show a semicircle, and the size is smaller than that of the intercalative $\text{LiNi}_{0.8}\text{Co}_{0.2}\text{O}_2$ electrode. This is considered neither a special example nor an experimental error, since the same tendency was obtained for the LiCoO_2 ablation electrode, as shown in Fig. 4.

The reason for not showing capacitive response is that the impedance measurement detects the motion of lithium atoms inside the film. A similar semicircular response in the low frequency region indicates that the intercalative and blocking electrodes are both related to lithium diffusion. When diffusion occurs, a straight line with a slope of 45° appears in the complex plane plot. However, no straight lines were observed for both electrodes. This observation suggests that the ideal lithium

diffusion or the chemical potential profile following Fick’s law does not occur inside these films. As one likely explanation, deviation from theoretical behavior is considered to stem from the thickness of the film. Since the thickness of the PLD films is in the order of several tens of nanometers, as identified by surface roughness measurements and X-ray reflectometry, the production of solid electrolyte interface (SEI) at the electrode surface must strongly influence the bulk process. It is, therefore, important to elucidate the real surface structure during intercalation and such research is now under way by Kanno and co-workers.

As a second explanation for not yielding a straight line, the mechanism of the diffusion should be considered. Lithium ions diffuse accompanied by electrons in the host matrix to maintain electrical neutrality. This paired motion of ion and electron should be taken into consideration. In addition, the speed of volumetric change or phase change in the host caused by lithium intercalation is also considered to influence the diffusion mechanism. Since the ablation film was quite thin and deposited on a substrate, the sliding or shifting of each layer may be anchored by the substrate surface and different from normal isolated electrode particles. In conclusion, the ablation film, in the absence of sufficient thickness, has the possibility to show different bulk properties compared to μm -order particles.

Fig. 5 shows the phase angle distribution as a function of the applied ac frequency. Each elemental process of intercalation can be clearly distinguished as an individual peak in this plot. Reactions occurring at the interface between the electrode and electrolyte appear in the frequency region above 1 Hz. They depend on the electrode-surface properties and do not depend on whether continuous current flows or not. In the case of intercalative orientation, there are two peaks located around 10^3 and 10^2 Hz, respectively.

On the other hand, the blocking electrode shows one peak around 10^3 Hz. This difference in the number of peaks is due to the different crystal orientation of the electrodes. The intercalative orientation of $\text{LiNi}_{0.8}\text{Co}_{0.2}\text{O}_2$ on $\text{STO}(1\ 1\ 0)$ has edge planes that are directed towards the electrolyte, while the blocking orientation presents basal planes. The peak around 10^3 Hz is common to both electrodes, and thus suggests a weak interaction between the electrode and ions in the electrolyte regardless of the crystal orientation. Another peak around 10^2 Hz appearing

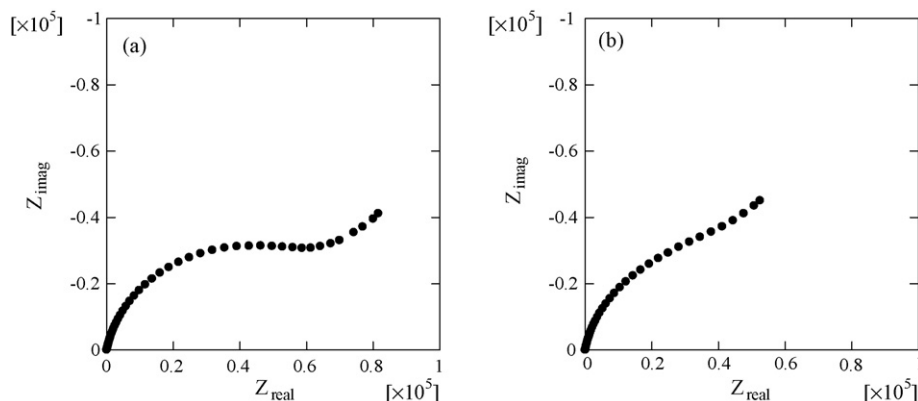


Fig. 4. Cole–Cole plots of LiCoO_2 ablation films on an STO substrate. (a) Intercalative film on $\text{STO}(1\ 1\ 0)$, and (b) blocking film on $\text{STO}(1\ 1\ 1)$.

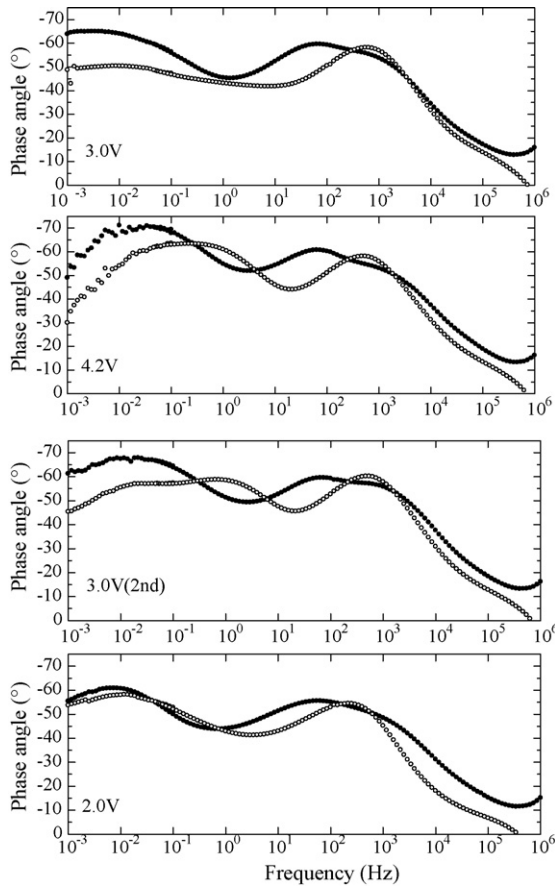


Fig. 5. Bode plots for $\text{LiNi}_{0.8}\text{Co}_{0.2}\text{O}_2$ films on $\text{STO}(110)$ and (111) substrates at different stages of intercalation. Open circles indicate the blocking film on $\text{STO}(111)$ and closed circles indicate the intercalative film on $\text{STO}(110)$.

only in the intercalative electrode shows a stronger relation to the edge surface, which may belong to ionic movement crossing the interface.

The temperature influence on these surface-reactions was also examined, and the temperature was varied from 20 to -20°C . The Bode plots obtained are shown in Fig. 6. The two peaks discussed in the previous paragraph show different degrees of dependence on the temperature. The peak at the lower frequency does not show much change, while that at the higher frequency shows a significant change due to the temperature

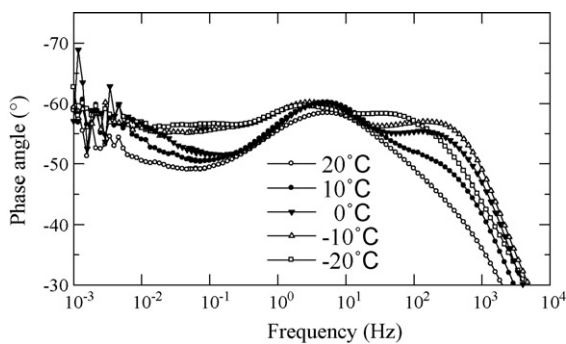


Fig. 6. Phase angle dependence on frequency at various temperatures for $\text{LiNi}_{0.8}\text{Co}_{0.2}\text{O}_2$ films on an $\text{STO}(110)$ substrate. The spectrum at 20°C is the same as the data at equilibrated at 3.0 V in Fig. 5.

variance. The elemental process at 10^3 Hz belongs to the reaction which directly reflects the nature of the electrolyte, since the electrolyte shows a rapid increase in viscosity near the freezing point. The peak at the lower frequency, which is less sensitive to the temperature, is considered to have the characteristics of a solid phase reaction. This is consistent with the consideration in the preceding paragraph that the peak at 10^2 Hz corresponds to ionic motion at the electrode interface.

Since STO is not a good electronic conductor, a gold substrate was used for comparison study. Laser ablation onto a polycrystalline gold sheet resulted in a dense blocking and polycrystalline $\text{LiNi}_{0.8}\text{Co}_{0.2}\text{O}_2$ film electrode. The charge-discharge test shows a similar profile as the powder electrode. A Cole-Cole plot and a Bode plot are shown in Fig. 7. The impedance plot shows the same response of a large semicircle as in the case of STO substrate. However, the size of the circle, that is, the entire resistance is reduced by about one order. On the other hand, the Bode plot shows two peaks around 10^3 and 10^1 Hz. These peaks are also

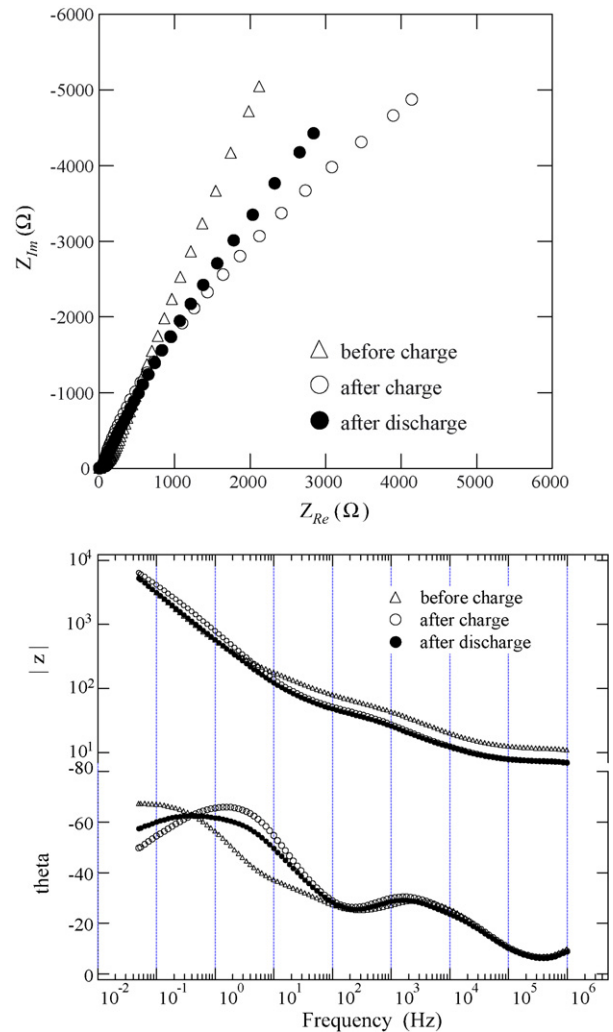


Fig. 7. Cole-Cole plots (upper figure) and Bode plots (lower figure) of the $\text{LiNi}_{0.8}\text{Co}_{0.2}\text{O}_2$ ablation film on the gold substrate. The spectra were obtained before charging, after full charging, and after full discharging. The film structure is characterized to be a blocking structure and polycrystalline. $|z|$ indicates the absolute resistance values of the impedance.

observed in the same regions when STO is used as a substrate in Fig. 5. Since the cell dimensions are almost similar, the reactions with the same time constant appear in the same frequencies. This result shows that the reaction mechanism of the $\text{LiNi}_{0.8}\text{Co}_{0.2}\text{O}_2$ ablation electrode is not changed by changing the substrate.

The electronic conductivity of the gold substrate increases the number of active sites on the electrode surface, however, the reaction itself on each site is not affected. It is concluded that the two surface reactions are intrinsic for the film and can be discussed as a characteristic feature of $\text{LiNi}_{0.8}\text{Co}_{0.2}\text{O}_2$.

4. Conclusions

Epitaxial polycrystalline films having different crystal orientations can provide information regarding the electrochemical response on specific crystal planes. Three elemental processes promoted by the presence of an electrical field were observed using a Cole–Cole plot and a Bode plot. The influence of the crystal orientation on electrochemical performance can be discussed with respect to these three processes. Among them, the bulk process appearing in the lowest frequencies needs further investigation for its deviation from the theoretical response. One of the other two processes is ionic transfer that occurs at the surface of the electrode. The other is considered to be the leakage current of the electric double layer. Wider application of ablation films in combination with impedance analysis will lead to quantitative discussion and elucidation of a more detailed mechanism of lithium intercalation.

Acknowledgements

This work was supported in part by a Grant-in-Aid for Scientific Research (B) “17350098” from the Ministry of Education, Culture, Sports, Science and Technology of Japan, and was also supported in part by a collaboration program with Mie University and Genesis Research Institute, Nagoya, Japan.

References

- [1] D. Mori, H. Oka, Y. Suzuki, N. Sonoyama, A. Yamada, R. Kanno, Y. Sumiya, N. Imanishi, Y. Takeda, *Solid State Ionics* 177 (2006) 535–540.
- [2] T. Kawada, K. Masuda, J. Suzuki, A. Kaimai, K. Kawamura, Y. Nigara, J. Mizusaki, H. Yugami, H. Arashi, N. Sakai, H. Yokokawa, *Solid State Ionics* 121 (1999) 271–279.
- [3] X. Chen, N. Wu, A. Ignatiev, Z. Shang, W.-K. Chu, *Thin Solid Films* 350 (1999) 130–137.
- [4] N. Imanishi, T. Matsumura, Y. Sumiya, K. Yoshimura, A. Hirano, Y. Takeda, D. Mori, R. Kanno, *Solid State Ionics* 174 (2004) 245–252.
- [5] H. Xia, L. Lu, G. Ceder, *J. Alloys Comp.* 417 (2006) 304–310.
- [6] P.J. Bouwman, B.A. Boukamp, H.J.M. Bouwmeester, P.H.L. Notten, *Solid State Ionics* 152/153 (2002) 181–188.
- [7] P.G. Bruce, M.Y. Saidi, *Solid State Ionics* 51 (1992) 187–190.
- [8] M. Itagaki, N. Kobari, S. Yotsuda, K. Watanabe, S. Kinoshita, M. Ue, *J. Power Sources* 148 (2005) 78–84.
- [9] B.A. Boukamp, *Solid State Ionics* 169 (2004) 65–73.
- [10] Y. Iriyama, M. Inaba, T. Abe, Z. Ogumi, *J. Power Sources* 94 (2001) 175–182.
- [11] Y. Iriyama, H. Kurita, I. Yamada, T. Abe, Z. Ogumi, *J. Power Sources* 137 (2004) 111–116.